Wavelets and Electromagnetics

Leo C. Kempel
Radiation Laboratory
Department of Electrical Engineering and Computer Science
University of Michigan, Ann Arbor, MI 48109-2122

December 19, 1991

Abstract

Wavelets are an exciting new topic in applied mathematics and signal processing. This paper will provide a brief review of wavelets which are also known as families of functions with an emphasis on interpretation rather than rigor. We will devise an indirect use of wavelets for the solution of integral equations based upon techniques adapted from image processing. Examples for resistive strips will be given illustrating the effect of these techniques as well as there promise in reducing dramatically the storage requirement in order to solve an integral equation for large bodies. We also will present a direct implementation of wavelets to solve an integral equation. Both methods suggest future research topics and may hold promise for a variety of uses in computational electromagnetics.

1 Introduction

Wavelets have generated significant excitement among applied mathematicians and engineers recently due to their unique properties and diversity. Wavelets are actually a family of basis functions which are generated by translation and dilation of a single function. The uses are diverse since many different wavelets may be generated which possess some properties which are particularly well suited for a given purpose. Three prominent uses of

wavelets are image compression which is discussed by Mallat([1],[2]) and Daubechies[3], solution of partial differential equations by the staff at Aware Inc.([4], [5]), and the solution of Fredholm Integral Equations by several members of the Yale research staff([6],[7],[8]).

This paper will give a brief and basic review of wavelets with an emphasis on the character of these functions rather than a rigorous mathematical treatment. Our purpose is to apply wavelet expansions or wavelet transforms to the solution of electromagnetic problems. We will show that a novel technique which is adopted from image processing may be applied to traditional Method of Moments(MoM) computer codes to achieve significant storage savings. Since modern computers are becoming increasingly fast, the primary limitation on MoM implementations is the $\mathcal{O}(N^2)$ storage requirement. The use of wavelets is intended to alleviate this requirement. This "image processing" technique may be used with existing MoM implementations to reduce storage. Finally we will look at direct applications of wavelets in electromagnetics with a modal solution of the Fredholm equation and discuss future research topics. Although we have only used E-polarized resistive strip examples for this paper these techniques are applicable to other electromagnetic problems of interest. In particular, although we only use MoM examples herein, we are interested in applying wavelet analysis in the solution of the boundary integral associated with the FEM-BE method.

2 Wavelets and Dilation Equations

Wavelets and their underlying form, a dilation equation, is an unfamiliar concept to most engineers. We will attempt to give a feel for what a wavelet is and what properties it possesses which are attractive for electromagnetics without going into detail. Strang[9] gave an excellent high-level review of the properties of wavelets while Daubechies[10] provides a rigorous review with significant new material. Mallat[2] was able to relate wavelet decomposition and reconstruction in terms of multiresolution analysis which allowed significant progress to be made in exploiting wavelets for the aforementioned applications.

In order to understand wavelets, we must first look at a dilation equation

$$\phi(x) = \sum_k c_k \phi(2x - k) \tag{1}$$

which is recognized as a two-scale difference equation. Strang[9] reviews the criterion which must be met in order for (1) to be unique. The "scaling function",$\phi(x)$, is determined recursively and thus many properties of it must be observed rather than defined. Daubechies[10] was able to construct orthonormal wavelets with compact support in both domains which was thought to be impossible by using the recursion

$$\phi_j(x) = \sum_k c_k \phi_{j-1}(2x-k) \tag{2}$$

with the box function as the fundamental function ($\phi_0(x)$) and certain simple conditions which determine c_k. The family of wavelets derived by Daubechies will be used for the examples of this paper although this is certainly not the only or necessarily optimal choice of wavelets.

At this point, we introduce the continuous wavelet family which comes from the scaling function,$\phi(x)$, as

$$\psi(x) = \sqrt{s}\phi(s(x-u)) \tag{3}$$

where the scale parameter(s) and the translation parameter(u) range over the positive real axis and the entire real axis, respectively (The notation adopted for the remainder of this paper is from Mallat [1]). A fundamental property of wavelets is their approximation capability. Daubechies family is denoted by the number of recursions used to determine the analyzing wavelet. For example we will denote the Daubechies wavelet which has four coefficients as DAUB4 which can recover up to a linear polynomial since the two lowest-order moment vanishes as discussed by Strang[9]. As terms are increased, more moments vanish and thus the polynomial approximation increases in order (e.g. DAUB6 will recover a quadratic).

As was previously mentioned, the Daubechies family is not only orthonormal but they enjoy the useful property of compact support. For example, figure 1 illustrates DAUB20 wavelet compared with the comparable cosine if we wish to represent an impulse "frequency" of $f = \frac{24}{1024\Delta}$ where Δ is the spatial sample size. As seen, the cosine(Fourier series basis) is compact in the "frequency" domain yet requires infinite support in the spatial domain. However, the Daubechies wavelet is compact in both domains. A further example is given in figure 2 where the excitation impulse is at $f = \frac{100}{1024\Delta}$ and we observe that as the "frequency" increases, the analyzing wavelet has

diminishing spatial support. This is the most important property of wavelets since finer spatial resolution is used for "high frequency" components which results in a more accurate evaluation than is possible for the comparable Fourier coefficient which is computed with constant sample size regardless of the "frequency".

Several groups ([4],[5],[6],[7], [8]) have recognized that the property of compact support in both domains will result in a sparse matrix when an integral operator is converted to a matrix operator. We will discuss in the next section the fact that if one thinks in terms of multiresolution analysis, the preceding observation is obvious.

3 Matrix Compression Techniques

One of the most promising applications of wavelets is image compression for the transmission and storage of detailed images. For example, The FBI is looking at using wavelet compression techniques in order to store their extensive finger print library without loss of fidelity. We will give a brief review of the wavelet transform, multiresolution analysis , and what this topic has to do with electromagnetics.

The continuous wavelet transform is given here without proof[1]

$$F(s,u) = \int_{-\infty}^{\infty} f(x)\psi_s(x-u)dx \tag{4}$$

where the wavelet family is given

$$\psi_s(x) = \sqrt{s}\psi(sx) \tag{5}$$

and $\psi(x)$ is the mother wavelet which is denoted as $\phi(x)$ in (8). In order to reconstruct a signal from its wavelet transform, we define the inverse wavelet transform as

$$f(x) = \int_{-\infty}^{\infty}\int_{0}^{\infty} F(s,u)\psi_s(x-u)dsdu \tag{6}$$

A more practical transform for numerical applications is the Discrete Wavelet Transform(DWT) which acts on a sequence of samples. In order to cover the phase-space, we need to uniformly sample the translation parameter while

exponentially sampling the scale parameter[1]. The resulting DWT is given

$$W_D[f(j,n)] = \int_{-\infty}^{\infty} f(x)\psi_{2^j}(u - n\alpha^{-j})dx \tag{7}$$

where α is the elementary dilation step. The signal may be reconstructed from its DWT by the series

$$f(x) = \sum_j \sum_n < f(u), \psi_{2^j}(u - n\alpha^{-j}) > \psi_{2^j}(u - n\alpha^{-j}) \tag{8}$$

with $< \cdot, \cdot >$ denoting the standard inner product. In practice, we choose $\alpha = 2$ for historical reasons although this is not necessary.

The Fourier transform is recognized as a transformation from the spatial domain to the wavenumber domain. However, the wavelet transform is a transformation from the spatial domain to the scale domain. This is the heart of the multiresolution interpretation of (7) as well as its fast implementation, the Fast Wavelet Transform(FWT). Each successive coefficient of the DWT describes the difference or details between the current level and a the previous decimated level. Figure 3 illustrates this concept. The first level, figure 3a, describes the smooth component of the signal. Each successive level adds detail to the reconstruction. Thus a smooth signal will have a large large-scale component and very small detail components which results in signal compaction. The efficiency of the FWT algorithm follows from the pyramid structure shown in figure 3. The highest detailed level (smallest-scale) requires that all samples be used in its computation. However each successive level requires half ($\alpha = 2$) the number of samples due to dilation which results in the FWT having the same order of operations as the FFT.

Mallat[2] was the first to recognize that this property naturally satisfies the procedure used in pyramid-encoding schemes. If one applies a two-dimensional FWT which is computed in a manner similar to the most common implementation of the two-dimensional FFT to an image, the image can be compressed into few large components and many components which are less than some tolerance whose omission does not adversely affect the fidelity of the image. Significant compression can occur depending on which analyzing wavelet is used.

We realized that the typical impedance matrix generated by a MoM code may be thought of as a complex-valued image! Thus it is reasonable to assume that we may apply the wavelet transform to a dense impedance matrix

to generate a sparse matrix. It should be mentioned that this technique is similar in concept to the Impedance Matrix Localization(IML) method proposed by Canning[11] who uses physical arguments to generate a transformation matrix which yields a sparse matrix by using sub-domain basis functions. It is not yet apparent which method yield superior results.

Suppose one wants to solve for the E-polarized scattering from a resistive strip. The appropriate integral equation is a Fredholm equation of the Second Kind

$$E_z^i(x,y) = R(x,y)J_z(x,y) + \frac{k_o}{4}\int_C J_z(x',y')H_o^{(1)}[k_o|\sqrt{(x-x')^2+(y-y'|)^2}]dl' \quad (9)$$

This may be solved numerically by converting the integral operator into a matrix operator via MoM to form the matrix equation

$$\mathbf{Z}J_z = E_z^i \quad (10)$$

where each entry of J_z and E_z^i corresponds to a spatial sample. If we look at the impedance matrix, $\mathbf{Z}$, typically it is dense. This is shown in figure 4 which is the impedance matrix generated by pulse basis-point matching on a 1λx1λ corner reflector where clearly all elements of this matrix are important.

If however we apply a wavelet transform to both sides of (10), we get the transformed equation in the scale-domain

$$\mathcal{Z}\mathcal{J}_z = \mathcal{E}_z^i \quad (11)$$

Figure 5 illustrates the matrix shown in figure 4 after wavelet transformation by the DAUB10 analyzing wavelet. Clearly, this matrix has fewer significant entries and is thus a sparse matrix. For images, edges tend to be very important thus we would use very compact (low-order) wavelets in order preserve these edges. However, when one has a smooth matrix such as the one shown in figure 4, smooth wavelets (large-order) will tend to have greater compaction capability than a small-order wavelet. In order to verify this claim, we looked at the compression realized by using different wavelets from the Daubechies family and a truncation tolerance of 10^{-2}. Table 1 summarizes the results of this study for the corner reflector when the matrix size was 32x32. We observe that the apparent storage was reduced to $\mathcal{O}$(20N) from N^2 without loss of fidelity as shown in figure 6. However, the large-order wavelets did not exhibit a significant advantage with respect to the small-order wavelets.

The reason for this unexpected result is the fact that the matrix in question is not large. A similar comparison is shown in table 2 for the case of a 6λ curved(inclusion angle = 45°) metallic strip which used a 128x128 impedance matrix. We recognize some advantage using large-order wavelets while maintaining fidelity as seen in figure 7. As a final example, we look at the simulation of a metallic half plane-linearly tapered resistive half plane junction which used a 1024x1024 matrix. A clear advantage using large-order wavelets is seen in table 3 where the apparent storage is reduced to $\mathcal{O}(70N)$ which results in a 93% storage savings without loss of fidelity as shown in figure 8!

The astute engineer will recognize the use of the term "apparent" in the preceding storage analysis. This is due to the fact that you need to generate the entire impedance matrix before transformation which results in $\mathcal{O}(N^2)$ storage. However, we have devised a simple block-by-block technique which will result in an actual memory savings. If one writes (10) as an augmented matrix equation where there are $(N/K)^2$ blocks of K^2 elements each where K is of course a power of two($\alpha = 2$) then we may write (11) as

$$\sum_{k=1}^{N/K} \mathcal{Z}_{lk}\mathcal{J}_k \;=\; \mathcal{E}_l \quad l = 1..N/K \tag{12}$$

To illustrate this technique, we looked at the junction simulation previously given. Table 4 compares the compression results realized when $K = 64$ and the tolerance was set at 10^{-4}. The total storage requirement is $K^2+\mathcal{O}(240N)$ which is a 75% storage savings compared to the original dense matrix. The degraded performance is due to that the fact that each block will require a large smooth component as well as detail components which are a result of the artificial boundaries created by the block method. It should be stressed that in spite of these artificial high components, fidelity is maintained as shown in figure 9. These observations are shown by comparing figure 10 and 11 which is the impedance matrix of a 4λ flat strip when the DAUB10 wavelet transform is applied on the entire matrix and in a block-by-block fashion with sixteen 32x32 blocks, respectively.

4 Integral Equations

The matrix compression technique described in the previous section is a rather indirect use of wavelets in electromagnetics. In this section, we will look at a more direct application of wavelets for the solution of integral equations. This method will not prove to be very useful but will provide a reference for future research.

The E-polarized scattering by a metallic strip may be solved by determining the current via the integral equation

$$E_z^i(x,y) = \frac{k_o}{4}\int_C J_z(x',y')H_o^{(1)}[k_o|\sqrt{(x-x')^2+(y-y')^2}|]dl' \tag{13}$$

where the integration domain, C, suggests the parameterization

$$\begin{aligned} x &= x(t) \\ y &= y(t) \end{aligned} \tag{14}$$

Thus (13) may be written

$$E_z^i(t) = \frac{k_o}{4}\int_{C_t} J_z(t')H_o^{(1)}[k_o|r(t,t')|]dt' \tag{15}$$

and

$$r(t,t') = \sqrt{(x(t)-x(t'))^2+(y(t)-y(t'))^2} \tag{16}$$

Let us now employ the method of weighted residuals using the discrete wavelet as an entire domain weight

$$\int_{C_t} E_z^i(t)\psi_{2^j}(t-m2^{-j})dt = \frac{k_o}{4}\int_{C_t}\int_{C_t} J_z(t')H_o^{(1)}[k_o|r(t,t')|]dt'\psi_{2^j}(t-m2^{-j})dt \tag{17}$$

If we now expand the unknown current in terms of wavelet basis(8) and realize that all of the resulting integrals are DWTs, we arrive at the matrix equation

$$\mathcal{Z}\mathcal{J}_z = \mathcal{E}_z^i \tag{18}$$

where now the impedance matrix is given directly by a two-dimensional DWT of the Hankel function of (17)

$$\mathcal{Z} = \mathcal{W}_D^2[H_o^{(1)}[k_o|r(t,t')|]] \tag{19}$$

and the unknown vector is composed of modal coefficients. This solution is analogous to finding a Fourier series expansion solution if the complex exponential is used rather than the wavelet. We also note that the scattered field is computed efficiently as

$$E_z^2 \sim \sqrt{\frac{2}{\pi k_o \rho}} e^{i(k_o \rho - \frac{\pi}{4})} \sum_{n=0}^{N-1} \left[-\frac{k_o}{4} \mathcal{E}_z^i(n) \mathcal{J}(n) \right] \tag{20}$$

where the excitation is computed via the FWT

$$\mathcal{E}_k^i = \mathcal{W}_D[e^{-ik_o[cos\phi x(t) + sin\phi y(t)]}] \tag{21}$$

Figure 12 illustrates that the aforementioned formulation does recover the solution for a 1λ metallic strip when 64 coefficients are determined. This is an unfortunately large number of terms required. The usefulness of this method does not improve with problem size as seen in figure 13 where even 1024 coefficients are not sufficient to characterize a 150λ strip. The failings of this particular formulation will be discussed in the next section.

5 Conclusions and Future Work

This paper has presented several different uses for wavelets or families of basis functions for computational electromagnetics. The relevant features and characteristics of wavelets were briefly discussed. Since the scope of this paper precludes a detailed review of wavelets, we mention that Strang[9] and Daubechies[10] give excellent reviews of wavelets. Mallat[1] not only introduces a particularly useful interpretation of wavelets and the wavelet transform, he developed from this viewpoint a quite efficient Fast Wavelet Transform which rivals the FFT in speed. Mallat also served to present this field in terms which are more accessible to engineers as compared the mathematicians "flavor" given by Daubechies.

We developed a novel technique adapted from image processing for generating a sparse matrix where previously a dense matrix was required. It should be stressed that the utility of this method solely is based of the scale characteristics of the impedance matrix rather than some restrictive mathematical operation such as convolution. The block-by-block compression method proposed resulted in significant storage savings. In the future, we are interested

in improving this method with respect to the degraded performance caused by block processing. It is reasonable to anticipate some improvement since only the most readily implemented techniques and analyzing wavelets were employed for this study and we understand the cause of the degradation. However it should be pointed out that if we can approach the efficiency of the entire matrix method, the block by block technique could be used with any existing code and a sparse matrix solver to dramatically extend the size of problems which could be handled with integral equation methods regardless of the geometry shape.

The second method looked at was a direct solution of the integral equation by wavelet expansion. This proved very disappointing. It is known that a Fourier series expansion of the current requires the retention of many terms. However, it was felt that the compact support property of wavelets would result in a dramatic reduction in the number of required coefficients. Although this initial trial did not succeed, we note that the wavelets chosen were available rather than the best possible. Further study may reveal more appropriate analyzing wavelets for our purpose or perhaps higher order wavelets are required for sufficient approximation.

Another avenue of research is employing wavelet testing with sub-domain basis functions. One may think of this operation as row-only compression rather than row and column compression which would result from the two-dimensional processing as described above. However, there would be no artificial components along the rows and by inspecting figure 11 we note that a significant amount of the spurious components are along rows of the matrix. This should result in a sparse matrix due to the local support of the basis and the compact support of the weights and a particularly appealing choice of basis are the ones used by Canning[11] since this basis will aid in compression along columns of the resulting matrix. To this date, we have not investigated this method. In addition, further study of Alpert *et al*[7] may yield further insight. It is noted that [7] investigated non-oscillating kernel functions while our kernel is certainly still a matter of research.

Wavelet processing and direct solution offers a promising avenue for extending integral equation techniques to much larger structures. It is noted that all methods described herein used FWT to evaluate all the integrals in an efficient manner. Although the examples presented involved the MoM, we are interested in using these techniques when terminating a Finite Element mesh with a boundary integral. An efficient solution in terms of unknowns

may be found for arbitrarily closures. This is in contrast the few available closures if one employs the CGFFT method to solve the boundary integral.

References

[1] Stephane G. Mallat, "Multifrequency Channel Decompositions of Images and Wavelet Models," *IEEE Trans. Acoust., Speech, Signal Processing*, Vol. 37, No. 12, pp. 2091-2110, Dec. 1989.

[2] Stephane G. Mallat, "A Theory for Multiresolution Signal Decomposition: The Wavelet Representation," *IEEE Trans. Acoust., Speech, Signal Processing*, Vol. 11, No. 7, pp. 674-693, July 1989.

[3] Ingrid Daubechies, "The Wavelet Transform, Time-Frequency Localization and Signal Analysis," *IEEE Trans. Info. Theory*, Vol. 36, No. 5, pp. 961-1005, Sept. 1990.

[4] Roland Glowinski, Wayne Lawton, Michel Ravachol, and Eric Tenenbaum, "Wavelet Solution of Linear and Nonlinear Elliptic, Parabolic, and Hyperbolic Problems in One Space Dimension," *Aware Inc. Tech. Report* AD890527.1, 1989.

[5] "Wavelet Analysis and the Numerical Solution of Partial Differential Equations," *Aware Inc. Tech. Report* AD900615.2, 1990.

[6] G. Beylkin, "On the Representation of Operators in Bases of Compactly Supported Wavelets," *pre-print.*

[7] B. Alpert, G. Beylkin, R. Coifman, and V. Rokhlin, "Wavelets for the Fast Solution of Second-Kind Integral Equations," *Yale Tech. Report* YALEU/DCS/RR-837, December 1990.

[8] G. Beylkin, R. Coifman, and V. Rokhlin, "Fast Wavelet Transforms and Numerical Algorithms I," *Comm. Pure Applied Math.*, 44:141-181, 1991.

[9] Gilbert Strang, "Wavelets and Dilation Equations: A brief introduction," *SIAM Review*,31(4):614-627, 1989.

[10] Ingrid Daubechies, "Orthonormal Bases of Compactly Supported Wavelets," *Comm. Pure Applied Math.*, 41:909-996, 1988.

[11] Francis X. Canning, "The Impedance Matrix Localization(IML) Method for Moment-Method Calculations," *IEEE Antennas and Propagat. Magazine*, pp. 18-30, October 1990.

Table 1

1 lambda Corner Reflector using 32 Unknowns and tol=10^-2

Wavelet	Zeros	Non-zeros	Total	Order
DAUB4	370	654	1024	20N
DAUB6	451	573	1024	20N
DAUB8	454	570	1024	20N
DAUB10	444	580	1024	20N
DAUB12	439	585	1024	20N
DAUB14	436	588	1024	20N
DAUB16	426	598	1024	20N
DAUB18	420	604	1024	20N
DAUB20	387	637	1024	20N

Table 2

6 lambda Curved Strip using 128 unknowns and tol=10^-2

Wavelet	Zeros	Non-zeros	Total	Order
DAUB4	10311	6073	16384	50N
DAUB6	12312	4072	16384	30N
DAUB8	13214	3170	16384	20N
DAUB10	13388	2996	16384	20N
DAUB12	13597	2787	16384	20N
DAUB14	13591	2793	16384	20N
DAUB16	13643	2741	16384	20N
DAUB18	13713	2671	16384	20N
DAUB20	13656	2728	16384	20N

Table 3

Resistive Junction using 1024 unknowns and tol=10^-4

Wavelet	Zeros	Non-zeros	Total	Order
DAUB4	573834	474742	1048576	460N
DAUB6	777806	270770	1048576	260N
DAUB8	871382	177194	1048576	170N
DAUB10	917716	130860	1048576	130N
DAUB12	940642	107934	1048576	110N
DAUB14	954802	93774	1048576	90N
DAUB16	966321	82255	1048576	80N
DAUB18	973085	75491	1048576	70N
DAUB20	978972	69604	1048576	70N

Tabel 4

Resistive Junction using block method w/ block size=64x64

Wavelet	Zeros	Non-zeros	Total	Order
DAUB4	268401	780175	1048576	760N
DAUB6	432037	616539	1048576	600N
DAUB8	569457	479119	1048576	470N
DAUB10	685377	363199	1048576	350N
DAUB12	744733	303843	1048576	300N
DAUB14	786832	261744	1048576	260N
DAUB16	796331	252245	1048576	250N
DAUB18	797724	250852	1048576	240N
DAUB20	799690	248886	1048576	240N

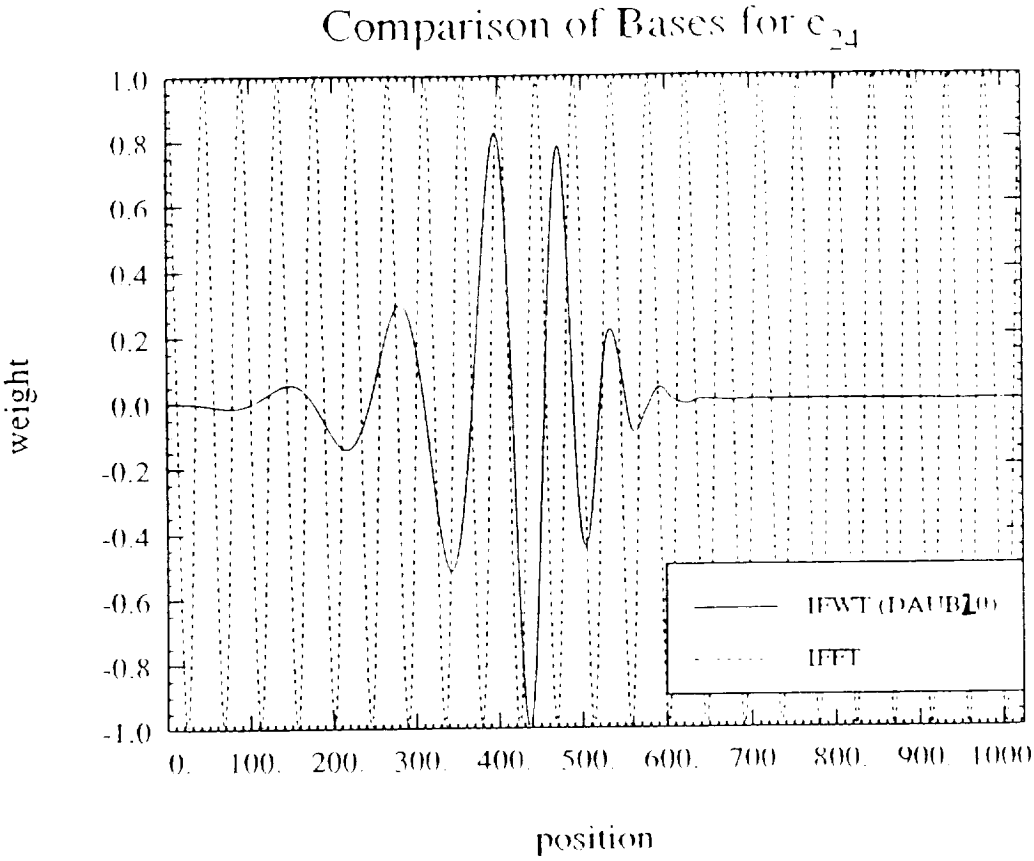
Comparison of Bases for e24
1.0
0.8
0.6
0.4
0.2
0.0
-0.2
-0.4
-0.6
-0.8
-1.0
weight
0.
100.
200.
300.
400.
500.
600.
700.
800.
900.
1000.
position
IEWT (DAUB10)
IFFT

Figure 1

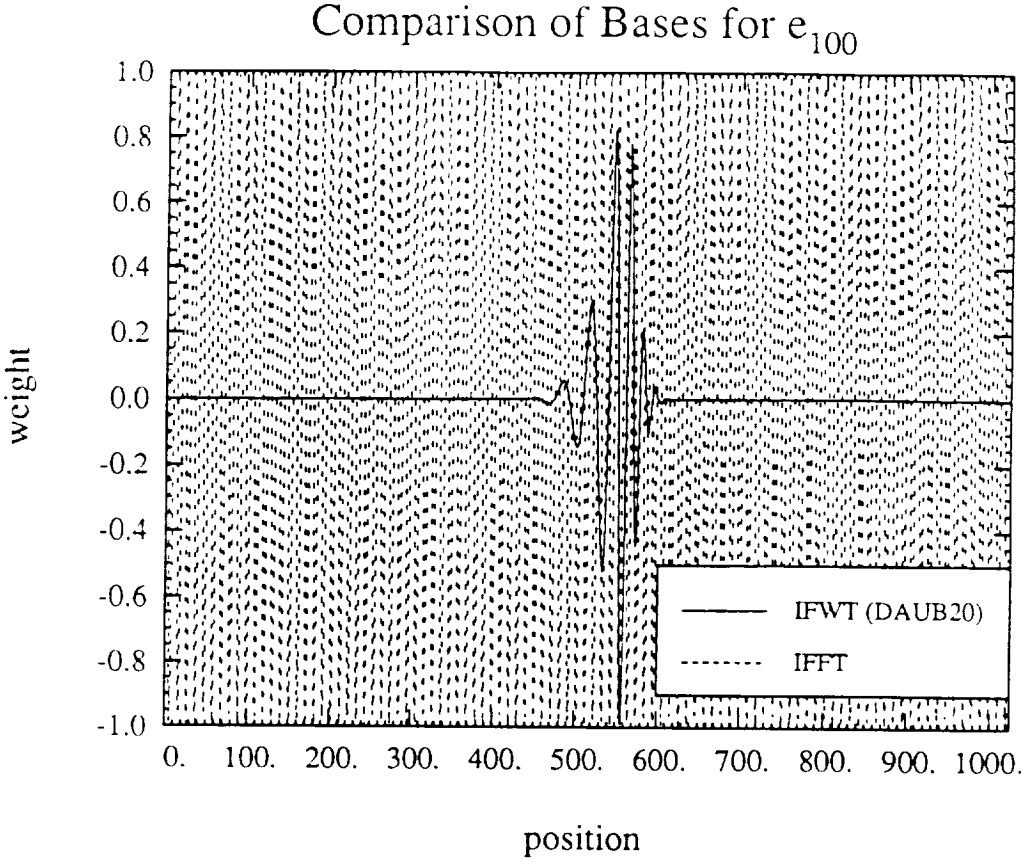
Comparison of Bases for e_{100}
1.0
0.8
0.6
0.4
0.2
0.0
-0.2
-0.4
-0.6
-0.8
-1.0
weight
0.
100.
200.
300.
400.
500.
600.
700.
800.
900.
1000.
position
IFWT (DAUB20)
IFFT

Figure 2

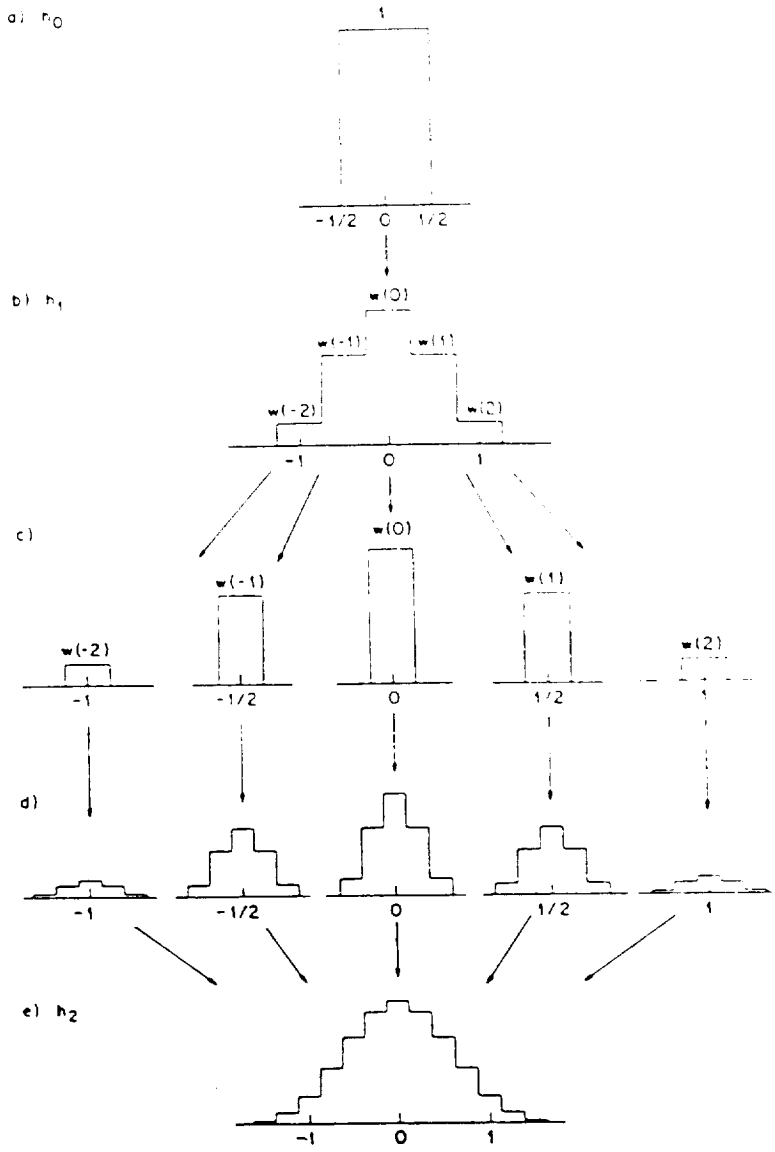

Figure 3. a) $h_0(x) = \chi_{[-1/2,1/2]}(x)$.

b) $h_1(x) = 2\sum w(n)\chi_{[n/2-1/4,\,n/2+1/4]}(x)$.

c) h_1 is decomposed into its "components"; each component is a multiple of the characteristic function of an interval of length $\frac{1}{2}$. (The "components" of h_j would have width 2^{-j}.)

d) Each "component" is replaced by a proportional version of h_1, centered around the same point as the component, and scaled down by a factor $\frac{1}{2}$. (This scaling factor would be 2^{-j} for h_j.)

e) The functions in d) are added to constitute h_2 (or h_{j+1}, if one starts from h_j in c)).

1λx1λ L-shaped Corner Reflector Impedance Matrix before Wavelet Transform

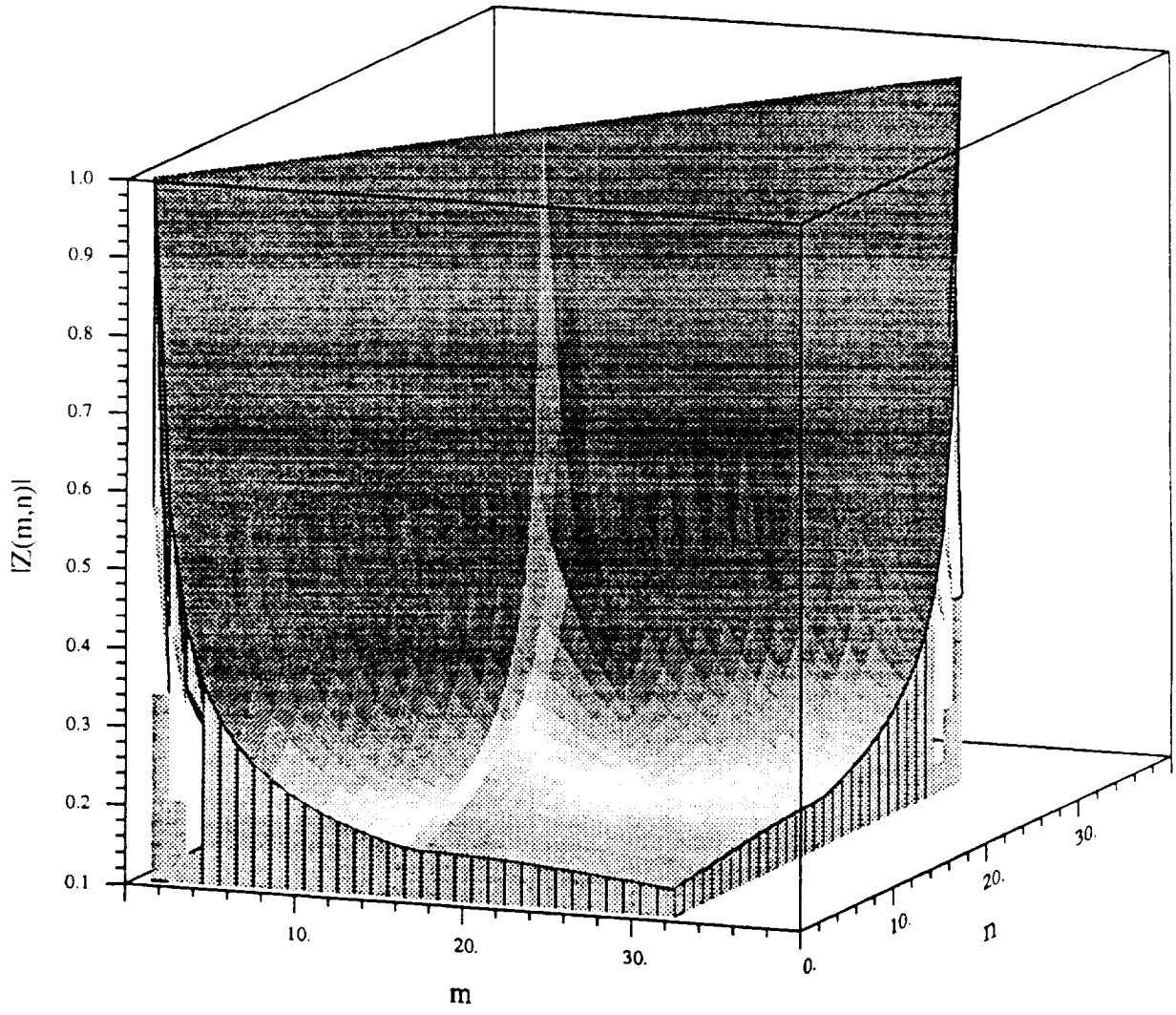

Figure 4

1λx1λ L-shaped Corner Reflector Impedance Matrix after DAUB10 Wavelet Transform

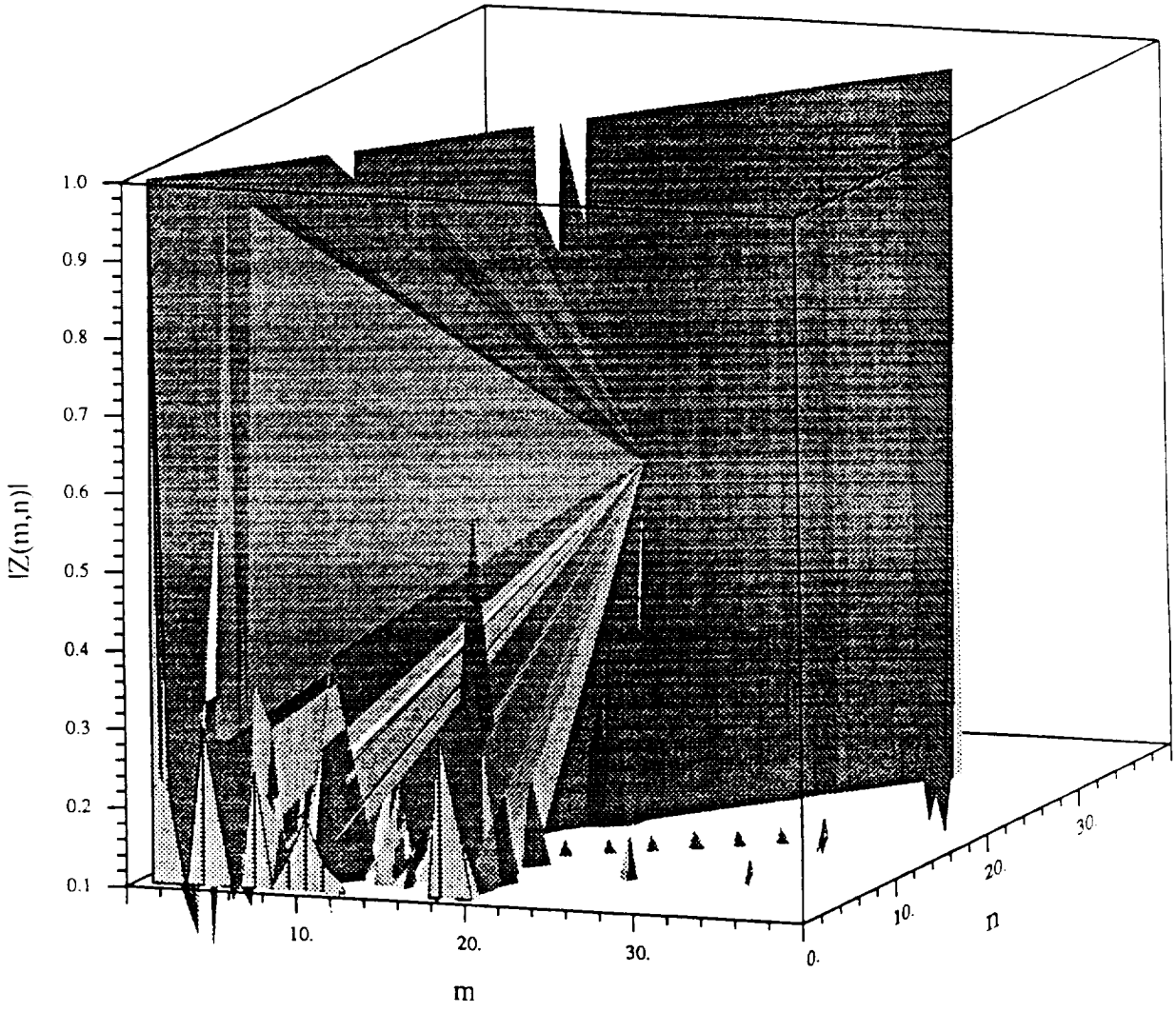

Figure 5

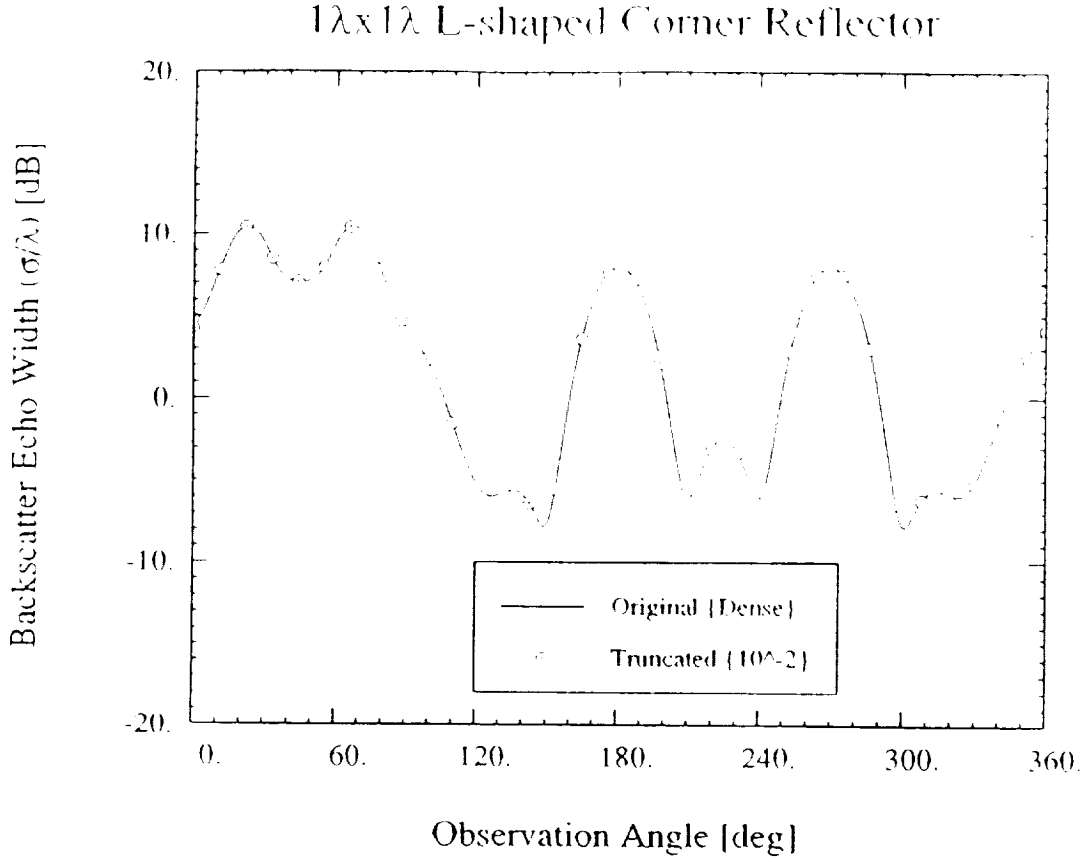
1λx1λ L-shaped Corner Reflector
Backscatter Echo Width (σ/λ) [dB]
20.
10.
0.
-10.
-20.
0.
60.
120.
180.
240.
300.
360.
Original (Dense)
Truncated (10^-2)
Observation Angle [deg]

Figure 6

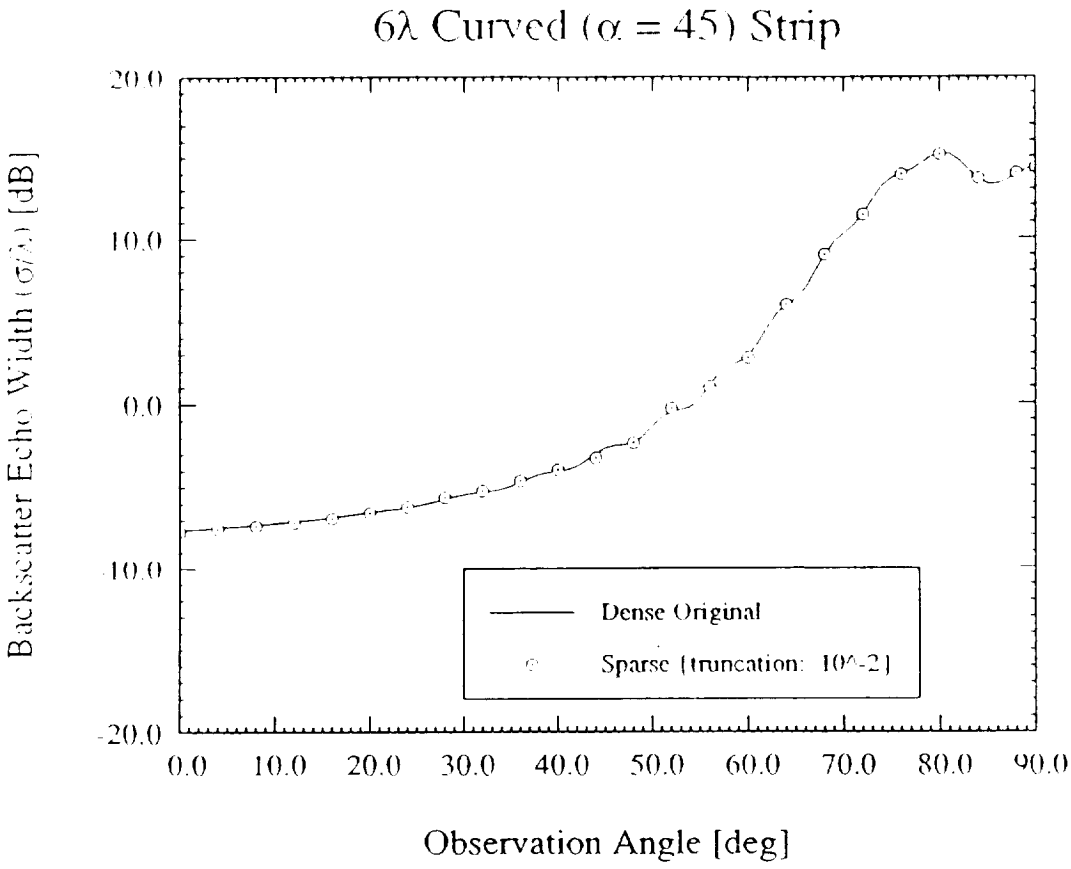
6λ Curved (α = 45) Strip
Backscatter Echo Width (σ/λ) [dB]
20.0
10.0
0.0
-10.0
-20.0
0.0
10.0
20.0
30.0
40.0
50.0
60.0
70.0
80.0
90.0
Dense Original
Sparse (truncation: 10^-2)
Observation Angle [deg]

Figure 7

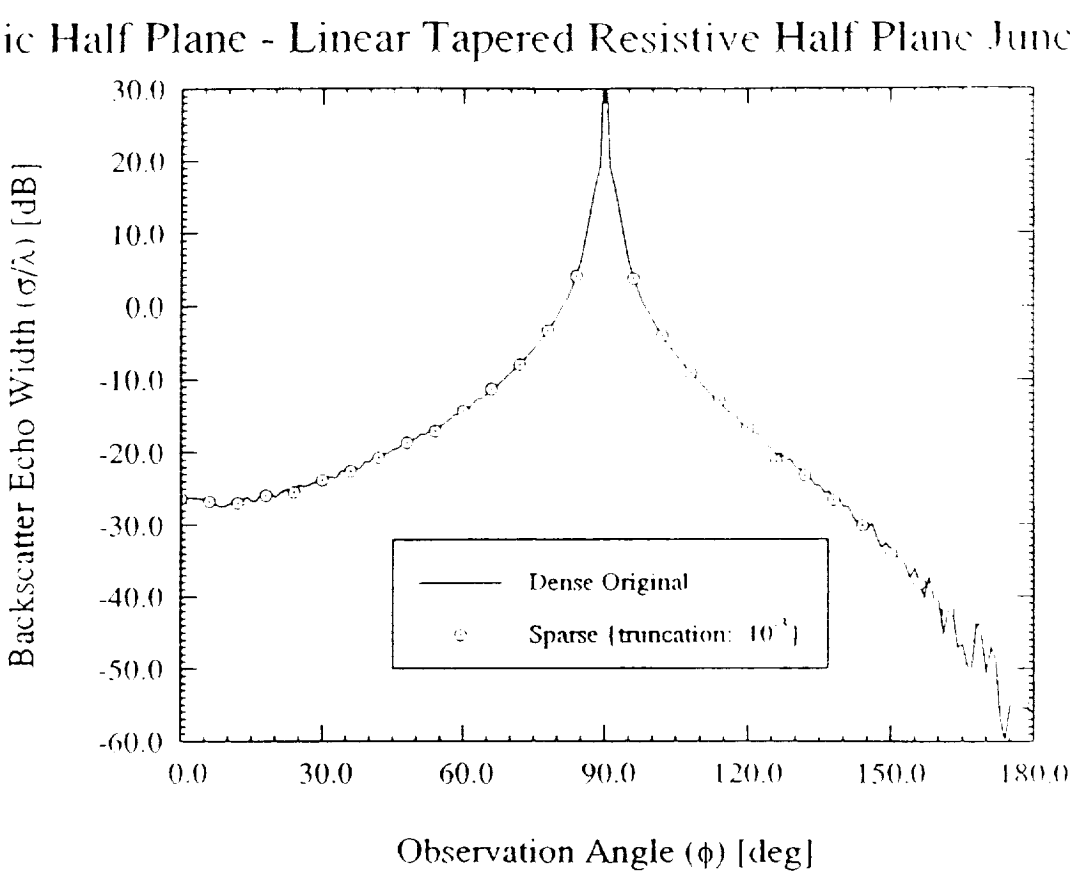
Metallic Half Plane - Linear Tapered Resistive Half Plane Junction (a_s = 1.0)
Backscatter Echo Width (σ/λ) [dB]
30.0
20.0
10.0
0.0
-10.0
-20.0
-30.0
-40.0
-50.0
-60.0
0.0
30.0
60.0
90.0
120.0
150.0
180.0
Dense Original
Sparse (truncation: 10^{-3})
Observation Angle (ϕ) [deg]

Figure 8

:tallic Half Plane - Linear Tapered Resistive Half Plane Junction ($a_2 = 1.0$)

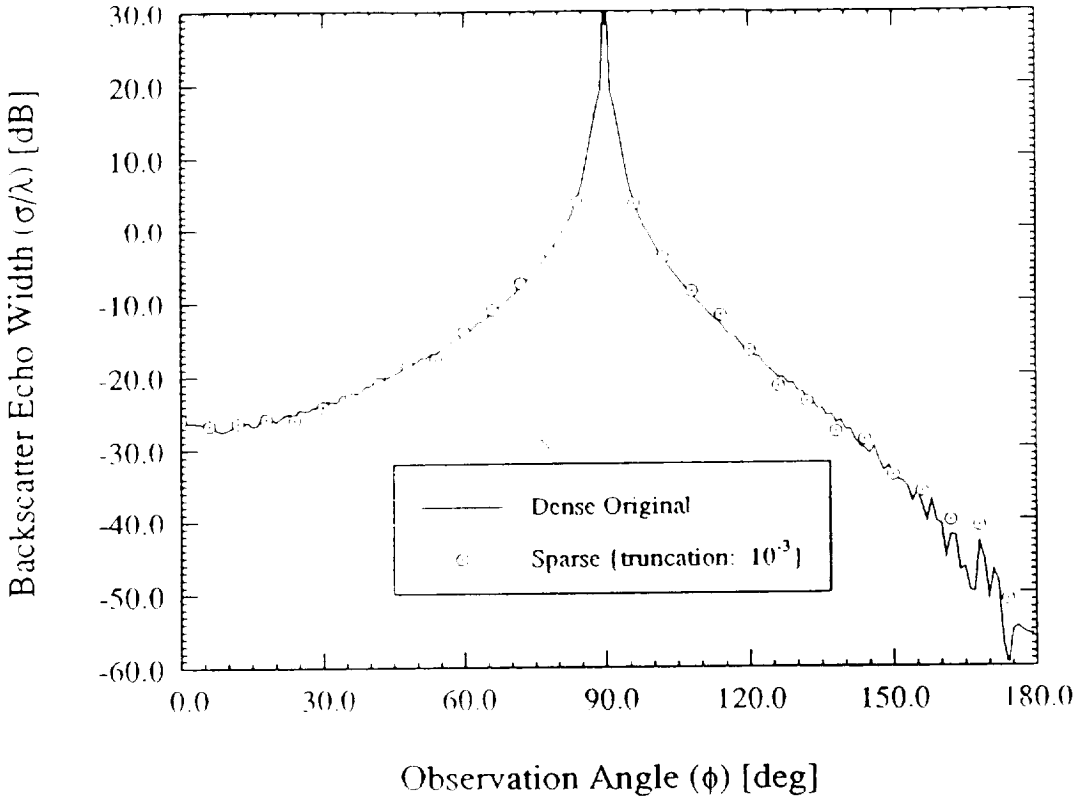

Figure 9

4λ Strip Impedance Matrix after Wavelet Transform performed all at once

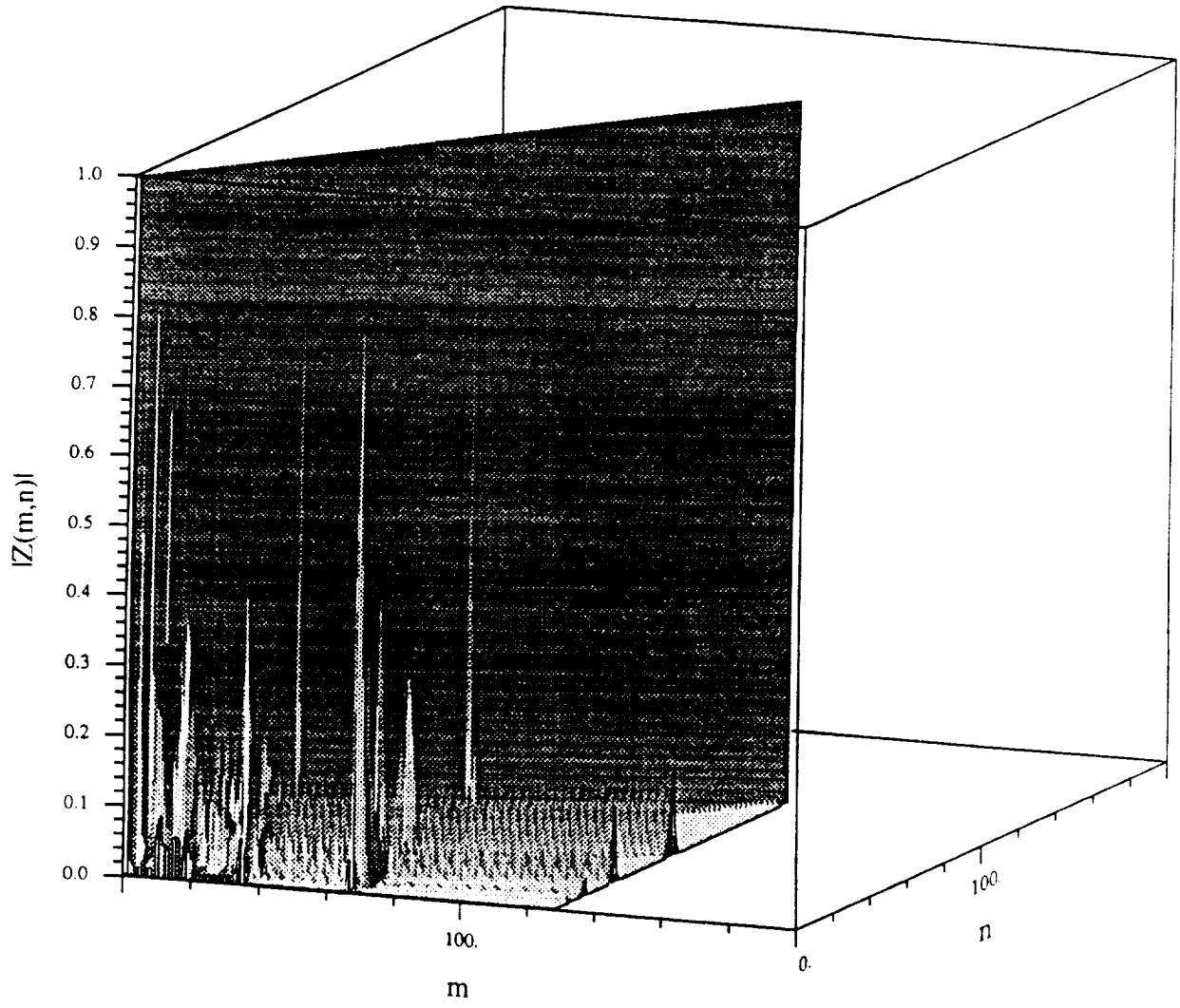

Figure 10

4λ Strip Impedance Matrix after Wavelet Transform performed block-by-block

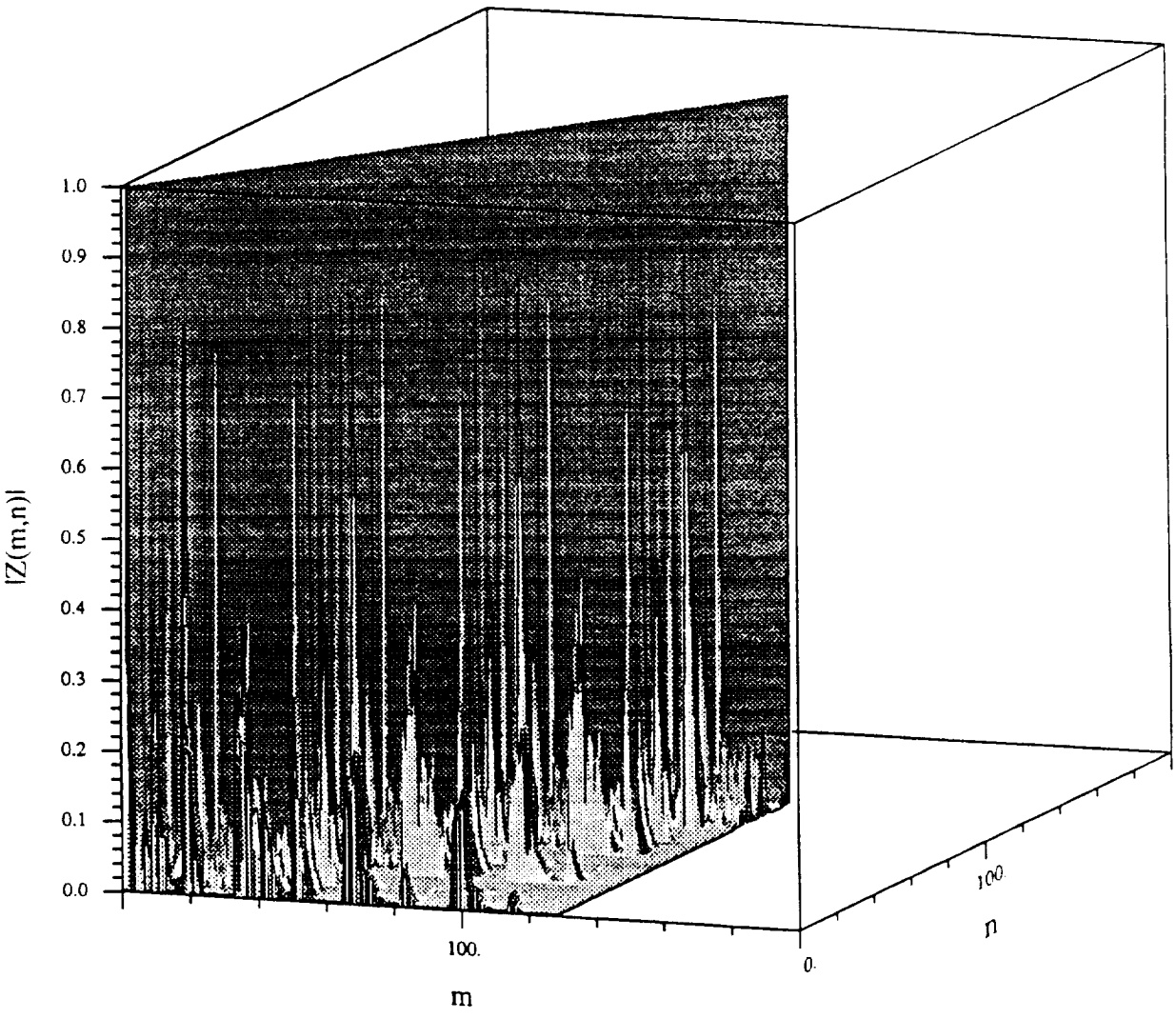

Figure 11

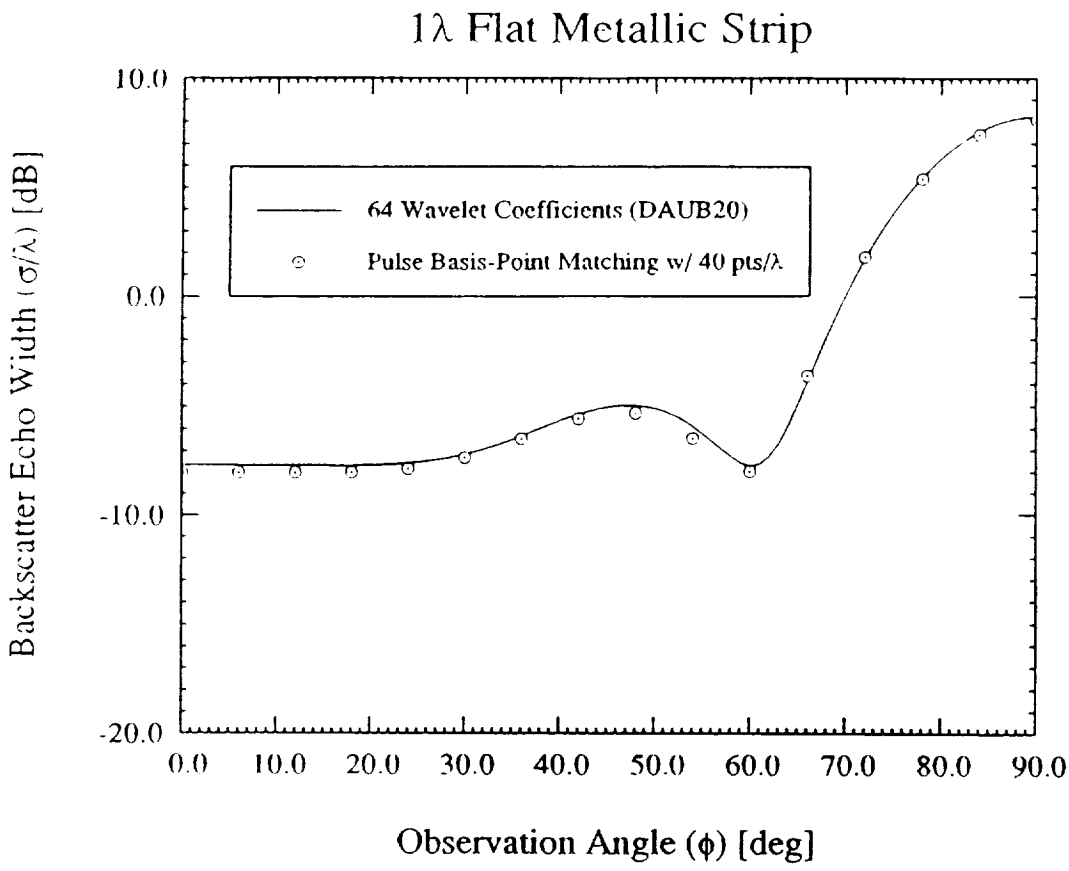
1λ Flat Metallic Strip
10.0
0.0
-10.0
-20.0
Backscatter Echo Width (σ/λ) [dB]
64 Wavelet Coefficients (DAUB20)
Pulse Basis-Point Matching w/ 40 pts/λ
0.0
10.0
20.0
30.0
40.0
50.0
60.0
70.0
80.0
90.0
Observation Angle (ϕ) [deg]

Figure 12

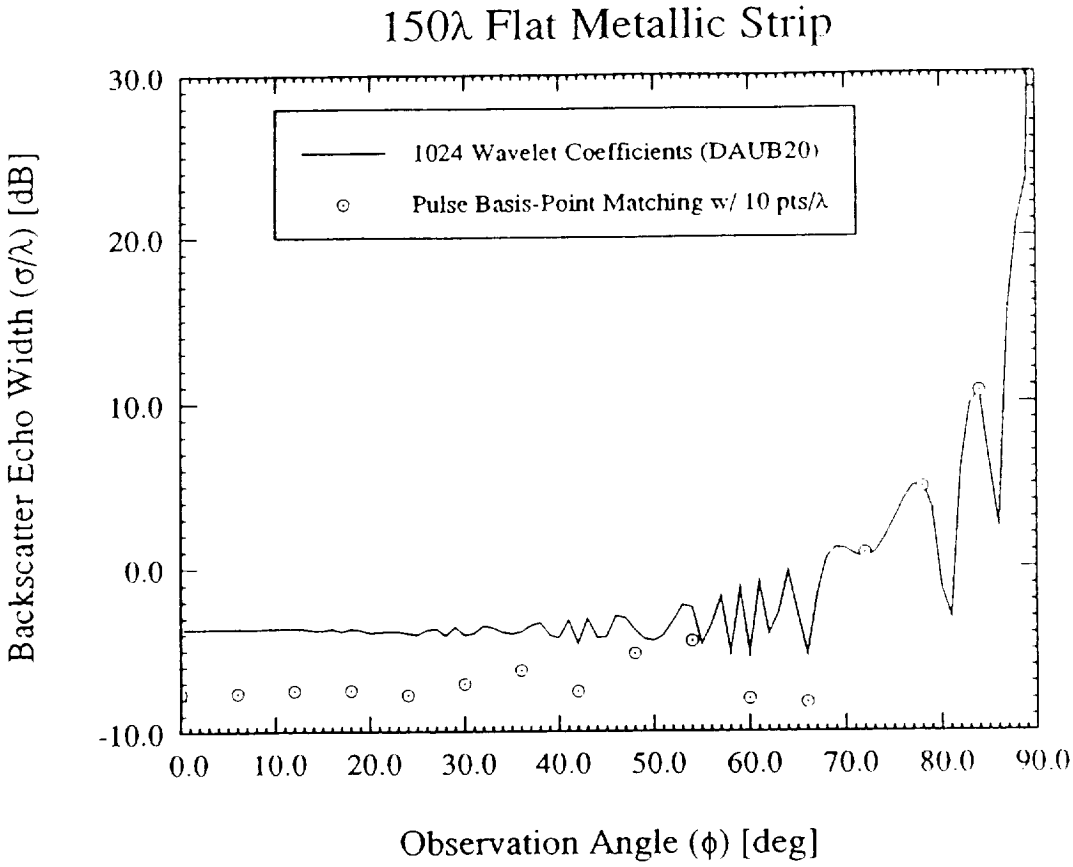
150λ Flat Metallic Strip
1024 Wavelet Coefficients (DAUB20)
Pulse Basis-Point Matching w/ 10 pts/λ
Backscatter Echo Width (σ/λ) [dB]
30.0
20.0
10.0
0.0
-10.0
0.0
10.0
20.0
30.0
40.0
50.0
60.0
70.0
80.0
90.0
Observation Angle (ϕ) [deg]

Figure 13